Journal of Hydrology 499 (2013) 200–209

Contents lists available at SciVerse ScienceDirect

Journal of Hydrology

journal homepage: www.elsevier.com/locate/jhydrol

Modeling contaminant transport in a two-aquifer system with an intervening aquitard

Chih-Tien Liu [a,1], Hund-Der Yeh [a,*], Li-Ming Yeh [b]

[a] Institute of Environmental Engineering, National Chiao Tung University, Hsinchu 300, Taiwan
[b] Department of Applied Mathematics, National Chiao Tung University, Hsinchu 300, Taiwan

ARTICLE INFO

Article history:
Received 26 January 2013
Received in revised form 1 June 2013
Accepted 26 June 2013
Available online 10 July 2013
This manuscript was handled by Peter K. Kitanidis, Editor-in-Chief, with the assistance of Todd C. Rasmussen, Associate Editor

Keywords:
Analytical solution
Finite difference solution
Aquitard
Laplace transform
de Hoog et al.'s method
Tauberian theorem

SUMMARY

This study deals with the issue of one-dimensional solute transport in a two-aquifer system, where an aquitard lies between two aquifers. Different from previous studies on analysis of the contaminant transport affected by the presence of an aquitard, we developed a mathematical transport model in an aquifer–aquitard–aquifer system with considering transport of solutes in the aquitard governed by both advection and diffusion. The Laplace-domain solution of the model for concentration distributions is obtained by the Laplace transform technique and its corresponding time-domain results are computed numerically by using Laplace numerical inversion. An explicit finite difference model is also developed to simulate two-dimensional contaminant transport process in the system. The simulated depth-averaged concentrations in the lower and upper aquifers slightly differ from those predicted by the present solution. The results show that the movement of contaminant in the upper aquifer is slowed down considerably due to the advective transport in aquitard. When neglecting the aquitard advection (a zero Peclet number), the concentration level in the lower aquifer will be underestimated, especially at late times. In addition, the contaminant concentration in the lower aquifer increases significantly with aquitard's Peclet number.

1. Introduction

Groundwater contamination from deliberate disposal or accidental spill of chemicals in aquifers has received much concern for the quality of water resources. It is rather complicated to analyze or predict the migration of contaminants in layered geologic formations analytically. Many aquifers with stratigraphic features are bounded above and/or below by low permeable layers, referred to as aquitards. Previous studies have demonstrated that the aquitard plays an important role in the behavior of subsurface flow and the migration of hazardous materials from underground storage tanks or industrial waste landfill (e.g., Johnson et al., 1989; Parker et al., 2004). The effect of the presence of an aquitard on the migration of contaminants is, however, commonly neglected or handled based on some simplifications from previous studies on flow and transport in stratigraphic formations. When the solutes migrate in an aquifer–aquitard–aquifer system, the solutes may penetrate the aquitard due to molecular diffusion. Furthermore, advective flux of solutes may also penetrate the aquitard due to the presence of hydraulic gradient produced by pumping in the adjacent aquifer (Cherry et al., 2006, p. 11) and/or other driving force such as concentration or temperature gradients (Freeze and Cherry, 1979, p. 25) between the aquifers. Thus, transport by advection in the aquitard might also be a significant transport process in the aquifer–aquitard–aquifer system and that desires consideration. Zhan et al. (2009a) mentioned that the advective flux in the aquitard should be considered in modeling contaminant transport if the aquitard is thin. For a thin aquitard, the solute may penetrate the aquitard and enter the adjacent aquifer. As such, it is of importance to include the contaminant transport in the adjacent aquifer in modeling contaminant transport in multilayered aquifer systems.

In the past, many studies had been devoted to analyze the effect of aquitards on groundwater flow systems. For instance, Hantush and Jacob (1955) assumed that the confined aquifer is bounded from below and above by aquitards of finite vertical extent in which flow is entirely vertical and the effect of the aquitard's elastic storage is negligible. In addition, the flow in the confined aquifer is essentially horizontal. From verification of the assumption of vertical flow in aquitards and horizontal flow in the aquifer, Neuman and Witherspoon (1969) concluded that "When the permeabilities of the aquifers are two or more orders of magnitude greater than that of the aquitard, errors introduced by this assumption are usually less than 5%". Zlotnik and Zhan (2005) and Hunt and Scott (2007) investigated the aquitard effect on the results of pumping tests by assuming that

* Corresponding author. Tel.: +886 3 5731910; fax: +886 3 5725958.
E-mail address: hdyeh@mail.nctu.edu.tw (H.-D. Yeh).
[1] Tel.: +886 3 5731910; fax: +886 3 5725958.

0022-1694/$ - see front matter © 2013 Elsevier B.V. All rights reserved.
http://dx.doi.org/10.1016/j.jhydrol.2013.06.050

a large conductivity contrast exists between the pumped aquifer and the aquitard, implying that the flow is horizontal in the pumped aquifer and vertical in the aquitard.

Diffusion at an aquifer–aquitard interface is somewhat similar to diffusion at a matrix-fracture boundary. It has been shown that matrix diffusion is an important process for contaminant transport in a fractured medium (Tang et al., 1981; Liu and Yeh, 2003; Liu et al., 2004). As a consequence, the advective flux in the aquitard has been neglected deliberately in previous analyses to make the derivation of analytical solutions tractable. Parker et al. (2004) showed that the migration of dissolved contaminants in low-permeability materials is typically dominated by molecular diffusion and may occur over time periods of hundreds to thousands years. Johns and Roberts (1991) proposed a model for investigating solute transport in large-aperture fractures under the consideration of lateral dispersion to the small aperture regions and diffusion to the rock matrix. Liu and Ball (2002) and Chapman and Parker (2005) recognized that back diffusion of the solute from the aquitard to the aquifer is the primary cause of the tailing effect observed in the aquifer. Note, however, that the solute transport by advection in aquitards was not taken into account in the above-mentioned studies. Zhan et al. (2009b) demonstrated that the mass transported between the aquifer and aquitard is sensitive to the aquitard's Peclet number, but less sensitive to the aquitard's diffusion coefficient, particularly at late times. In addition to the diffusive flux, their results implied that the advective flux in the aquitard is an important transport process for the contaminant to penetrate through the aquitard.

The objective of this paper is to develop a new mathematical model to describe contaminant transport in an aquifer–aquitard–aquifer system. Different from previous studies, this model considers the migration of contaminants by both advection and diffusion processes in the aquitard. The solution of the model in the Laplace domain is developed using Laplace transforms with the aid of both Ferrari's solution and Cardan's solution (Korn and Korn, 2000) and its corresponding results in the time domain are computed by de Hoog et al.'s algorithm (1982). The steady-state solution is also obtained from the Laplace-domain solution through the use of Tauberian theorem (Yeh and Wang, 2007). The concentrations predicted from this new solution are compared with the simulated depth-averaged concentrations from a two-dimensional explicit finite-difference model. Those newly developed solutions quantify the contaminant transport in an aquifer–aquitard–aquifer system and can be used to analyze the influences of aquitard properties on contaminant transport.

2. Conceptual and mathematical model

2.1. Conceptual model

Many aquitards exhibit variations in thickness or major internal lithology and therefore are often discontinuous in geologic facies at the regional scale. Cherry et al. (2006) presented a series of conceptual models for aquitards due to variations in depositional settings and post-depositional processes. Fig. 1 shows the schematic representation of the problem investigated in this study. The origin is located at the lower left-hand corner of the upper aquifer. The arrow shows the groundwater flow direction in both aquifers. Advection and diffusion are the physical processes controlling the transport of contaminants from the upper aquifer to the lower one through the aquitard.

2.2. Mathematical model

The assumptions related to the geometry and hydraulic properties of an aquifer–aquitard–aquifer system in the conceptual model are made as follows:

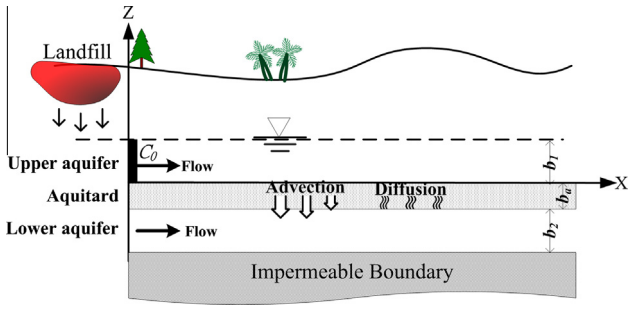

Fig. 1. Schematic representation of two-aquifer systems.

1. The flow and transport in both aquifers and aquitard is one dimensional. In addition, the flow fields are steady and uniform in the both aquifers and aquitard.
2. The hydraulic conductivity of the aquitard is a few orders of magnitude less than those of two adjacent aquifers, thus the direction of advective flow in the aquitard is vertical, i.e., perpendicular to the interface.
3. The aquifers and aquitard are homogeneous and isotropic with constant dispersivities and retardation factor.
4. The contaminants with a concentration kept constant at the inlet enter the two-aquifer system through the left boundary of the upper aquifer, while the lower one is initially not contaminated.

Based on these assumptions, the governing equations and associated initial and boundary conditions for the upper aquifer, aquitard, and lower aquifer are given below:

For the upper aquifer,

$$\frac{\partial C_1}{\partial t} = \frac{D_1}{R_1}\frac{\partial^2 C_1}{\partial x^2} - \frac{v_1}{R_1}\frac{\partial C_1}{\partial x} - \frac{\Gamma_1}{\theta_1 b R_1} \tag{1}$$

$$\Gamma_1 = \theta_a\left(v_a C_a - D_a\frac{\partial C_a}{\partial z}\right)\Big|_{z=0} \tag{2}$$

$$C_1(x,0) = 0 \tag{3}$$

$$C_1(0,t) = C_0 \tag{4}$$

$$C_1(\infty,t) = 0 \tag{5}$$

where C_1 and C_a represent the contaminant concentration in the upper aquifer and the aquitard, respectively; C_0 is the constant concentration at $x = 0$; v_1 is the average horizontal velocities of groundwater flow in the upper aquifer; v_a is the vertical velocity of groundwater flow in the aquitard; D_1 is the longitudinal dispersion coefficients for the upper aquifer and defined as $D_1 = \alpha_L v_1 + D^*$ with the longitudinal dispersivity α_L and the molecular diffusion coefficient in water D^*; D_a is the diffusion coefficient for the aquitard and defined as $D_a = \tau D^*$ with aquitard tortuosity τ; variable b is the half thickness of the aquifers; θ_1 and θ_a are the porosities of the upper aquifer and the aquitard, respectively; R_1 is the retardation factor in the upper aquifer, and t is elapsed time.

For the aquitard,

$$\frac{\partial C_a}{\partial t} = \frac{D_a}{R_a}\frac{\partial^2 C_a}{\partial z^2} - \frac{v_a}{R_a}\frac{\partial C_a}{\partial z} \tag{6}$$

$$C_a(x,z,0) = 0 \tag{7}$$

$$C_a(x,0,t) = C_1(x,t) \tag{8}$$

$$C_a(x,-b_a,t) = C_2(x,t) \tag{9}$$

where b_a and R_a are the thickness and the retardation factor of the aquitard, respectively. And for the lower aquifer,

$$\frac{\partial C_2}{\partial t} = \frac{D_2}{R_2}\frac{\partial^2 C_2}{\partial x^2} - \frac{v_2}{R_2}\frac{\partial C_2}{\partial x} + \frac{\Gamma_2}{\theta_2 b R_2} \tag{10}$$

$$\Gamma_2 = \theta_a\left(v_a C_a - D_a\frac{\partial C_a}{\partial z}\right)\Big|_{z=-b_a} \tag{11}$$

$$C_2(x,0) = 0 \tag{12}$$

$$C_2(0,t) = 0 \tag{13}$$

$$C_2(\infty,t) = 0 \tag{14}$$

where C_2 represents the contaminant concentration in the lower aquifer; v_2 is the average horizontal velocities of groundwater flow in the lower aquifer; D_2 is the longitudinal hydrodynamic dispersion coefficients for the lower aquifer, and defined as $D_2 = \alpha_L v_2 + D^*$. In addition, θ_2 and R_2 are the porosities and the retardation factor in the lower aquifer, respectively.

Eq. (2) represents the total flux crossing the interface between the upper aquifer and the aquitard. Similarly, Eq. (11) denotes the total flux through the aquitard and the lower aquifer (Zhan et al., 2009a). Eqs. (8) and (9) represent the continuities of concentrations at the upper and lower aquifer–aquitard interfaces, respectively.

2.2.1. Laplace-domain solutions

In the following, the Laplace-domain solutions to the governing equations (i.e., Eqs. (1), (6), and (10)) are developed. Using the dimensionless parameters listed in Table 1, Eqs. (1)–(14) can be expressed in dimensionless forms. Transforming Eqs. (1)–(14) into dimensionless form and applying the Laplace transform to the governing equations and boundary conditions results in the following equation groups:

For the upper aquifer,

$$\frac{d^2\overline{C}_{1D}}{dx_D^2} - Pe_1\frac{d\overline{C}_{1D}}{dx_D} - \varepsilon_1\overline{C}_{1D} + \kappa_1\frac{d\overline{C}_{aD}}{dz_D} = p\overline{C}_{1D} \tag{15}$$

$$\overline{C}_{1D}(0,p) = \frac{1}{p} \tag{16}$$

$$\overline{C}_{1D}(\infty,p) = 0 \tag{17}$$

For the aquitard,

$$\frac{d^2\overline{C}_{aD}}{dz_D^2} - Pe_a\frac{d\overline{C}_{aD}}{dz_D} = \delta_1 p\overline{C}_{aD} \tag{18}$$

$$\overline{C}_{aD}(0,p) = \overline{C}_{1D}(x_D,p) \tag{19}$$

$$\overline{C}_{aD}(-1,p) = \overline{C}_{2D}(x_D,p) \tag{20}$$

And for the lower aquifer,

$$\frac{d^2\overline{C}_{2D}}{dx_D^2} - Pe_2\frac{d\overline{C}_{2D}}{dx_D} + \varepsilon_2\overline{C}_{2D} - \kappa_2\frac{d\overline{C}_{aD}}{dz_D} = \delta_2 p\overline{C}_{2D} \tag{21}$$

Table 1
Dimensionless parameters used in the study.

$x_D = \frac{x}{b}$, $z_D = \frac{z}{b_a}$, $t_D = t\frac{D_1}{R_1 b^2}$, $C_{1D} = \frac{C_1}{C_0}$, $C_{2D} = \frac{C_2}{C_0}$, $C_{aD} = \frac{C_a}{C_0}$
$Pe_1 = \frac{v_1 b}{D_1}$, $Pe_2 = \frac{v_2 b}{D_2}$, $Pe_a = \frac{v_a b_a}{D_a}$, $\varepsilon_1 = \frac{\theta_a v_a b}{\theta_1 D_1}$, $\varepsilon_2 = \frac{\theta_a v_a b}{\theta_2 D_2}$, $\kappa_1 = \frac{\theta_a D_a b}{\theta_1 D_1 b_a}$
$\kappa_2 = \frac{\theta_a D_a b}{\theta_2 D_2 b_a}$, $\delta_1 = \frac{R_a}{R_1}\frac{D_1}{D_a}\left(\frac{b_a}{b}\right)^2$, $\delta_2 = \frac{R_2}{R_1}\frac{D_1}{D_2}$

$$\overline{C}_{2D}(0,p) = 0 \tag{22}$$

$$\overline{C}_{2D}(\infty,p) = 0 \tag{23}$$

where p is the Laplace variable.

The detailed development of the solutions in the Laplace domain describing the concentration distributions in the upper aquifer, aquitard, and lower aquifer is given in Appendix A. It is important to recognize that the governing equation for the lower aquifer becomes a linear fourth-order ordinary differential equation (ODE) when coupling the Laplace-domain solution with the upper one, $\overline{C}_{1D}(x_D,p)$.

The fourth-order ODE can be transformed to a quartic algebraic characteristic equation (Kreyszig, 1979). This quartic equation can be reduced to a cubic equation by applying Ferrari's solution and reduced further to two quadratic equations using Cardan's solution (Korn and Korn, 2000). The roots of the quartic equation can be determined from those two quadratic equations. Finally, the Laplace-domain solution for the lower aquifer can be found from the general solution of the fourth-order ODE with associated boundary conditions.

The final result of the dimensionless concentration in Laplace domain in the upper aquifer is given by

$$\overline{C}_{1D}(x_D,p) = \frac{1+\Lambda_1}{p}\exp(s_2 x_D) - \frac{\Lambda_1\cos(\beta_2 x_D) - \Lambda_2\sin(\beta_2 x_D)}{p} \times \exp(v_2 x_D) \tag{24}$$

with

$$\Lambda_1 = \frac{h_1 h_2}{[\beta_2^2+(v_2-s_1)^2][\beta_2^2+(v_2-s_2)^2]}\frac{2v_2-Pe_1}{2v_2-Pe_2}$$

$$\Lambda_2 = \frac{h_1 h_2}{[\beta_2^2+(v_2-s_1)^2][\beta_2^2+(v_2-s_2)^2]}\frac{v_2(v_2-Pe_1)-\beta_2^2-g_1}{\beta_2(2v_2-Pe_2)}$$

where

$$h_1 = \kappa_1\beta_0\exp(v_0)/\sin h(\beta_0); \quad h_2 = \kappa_2\beta_0\exp(-v_0)/\sin h(\beta_0);$$
$$g_1 = 0.5\varepsilon_1 - \kappa_1\beta_0/\tan h(\beta_0) + p;$$

$$g_2 = 0.5\varepsilon_2 + \kappa_2\beta_0/\tan h(\beta_0) - \delta_2 p; \quad s_1 = v_1 + \beta_1;$$
$$s_2 = v_1 - \beta_1; \quad v_0 = Pe_a/2;$$

$$v_2 = (Pe_1 + Pe_2 - 2\sqrt{\mu})/4; \quad \beta_0 = \sqrt{v_0^2 + \delta_1 p};$$
$$\beta_1 = \sqrt{v_1^2 + g_1}; \text{ and}$$

$$\beta_2 = \sqrt{\mu + 2o_1 - 2q_1\mu^{-1/2}} \quad \text{with}$$

$$\mu = \left(-q_2/2 + \sqrt{(q_2/2)^2 + (o_2/3)^3}\right)^{\frac{1}{3}} + \left(-q_2/2 - \sqrt{(q_2/2)^2 + (o_2/3)^3}\right)^{\frac{1}{3}} - 2o_1/3;$$

$$o_2 = -4r_1 - o_1^2/3; \quad q_2 = 8r_1 o_1/3 - 2\cdot(o_1/3)^3 - q_1^2;$$

$$o_1 = Pe_1 Pe_2/4 - 3(Pe_1^2 + Pe_2^2)/8 - g_1 + g_2;$$

$$q_1 = (Pe_2 - Pe_1)(g_1+g_2)/2 + Pe_1 Pe_2(Pe_1+Pe_2)/8 - (Pe_1^3 + Pe_2^3)/8;$$

$$r_1 = (Pe_2 g_1 - Pe_1 g_2)(Pe_1+Pe_2)/4 - (g_1 g_2 + h_1 h_2) - (g_1 - g_2 - Pe_1 Pe_2)(Pe_1+Pe_2)^2/16 - 3(Pe_1+Pe_2)^4/256.$$

The Laplace-domain solution of the dimensionless concentration in the aquitard has the form

$$\overline{C}_{aD}(x_D,z_D,p)=\frac{\exp(v_0 z_D)}{\sin h(\beta_0)}(\sin h(\beta_0(1+z_D))\overline{C}_{1D}-\exp(v_0)\times \sin h(\beta_0 z_D)\overline{C}_{2D}) \quad (26)$$

Finally, the Laplace-domain solution of the dimensionless concentration in the lower aquifer is

$$\overline{C}_{2D}(x_D,p)=\frac{h_2}{\beta_2(2v_2-Pe_2)\cdot p}\exp(v_2 x_D)\sin(\beta_2 x_D) \quad (27)$$

2.2.2. Steady-state solution

The steady-state solution for the dimensionless concentration distributions in the aquifers and aquitard can be obtained by applying the Tauberian theorem, also called the Final Value theorem, to Eqs. (24), (26), and (27). The development of the steady-state solution for the dimensionless concentration distributions in the upper aquifer, aquitard, and lower aquifer is given in Appendix B. The result for the upper aquifer is

$$C_{1D}=(1+\Omega_1)\exp(s_4 x_D)-[\Omega_1\cos(\beta_3 x_D)-\Omega_2\sin(\beta_3 x_D)]\times\exp(v_3 x_D) \quad (28)$$

with

$$\Omega_1=\frac{h_3 h_4}{(\beta_3^2+(v_3-s_3)^2)(\beta_3^2+(v_3-s_4)^2)}\cdot\frac{2v_3-Pe_1}{2v_3-Pe_2}$$

$$\Omega_2=\frac{h_3 h_4}{(\beta_3^2+(v_3-s_3)^2)(\beta_3^2+(v_3-s_4)^2)}\cdot\frac{v_3(v_3-Pe_1)-\beta_3^2-g_3}{\beta_3(2v_3-Pe_2)}$$

where

$$h_3=-\kappa_1 v_0\exp(-v_0)/\sin h(v_0);\quad h_4=-\kappa_2 v_0\exp(-3v_0)/\sin h(v_0);\quad g_3=\varepsilon_1-h_3;$$

$$g_4=\varepsilon_2+h_4;\quad s_3=Pe_1/2+\sqrt{(Pe_1/2)^2+g_3};\quad s_4=Pe_1/2-\sqrt{(Pe_1/2)^2+g_3};$$

$$v_3=(Pe_1+Pe_2-2\sqrt{\mu'})/4;\quad \beta_3=\sqrt{\mu'+2o_1'-2q_1'(\mu')^{-1/2}}\Big/2;$$

$$\mu'=\left(-q_2'/2+\sqrt{(q_2'/2)^2+(o_2'/3)^3}\right)^{\frac{1}{3}}+\left(-q_2'/2-\sqrt{(q_2'/2)^2+(o_2'/3)^3}\right)^{\frac{1}{3}}-2o_1'/3;$$

$$o_2'=-4r_1'-o_1'^2/3;\quad q_2'=8r_1'o_1'/3-2\cdot(o_1'/3)^3-q_1'^2;\quad o_1'=Pe_1Pe_2/4-3(Pe_1^2+Pe_2^2)/8-g_1'+g_2';$$

$$q_1'=(Pe_2-Pe_1)(g_1'+g_2')/2+Pe_1Pe_2(Pe_1+Pe_2)/8-(Pe_1^3+Pe_2^3)/8;$$

$$r_1'=(Pe_2g_1'-Pe_1g_2')(Pe_1+Pe_2)/4-(g_1'g_2'+h_1'h_2')-(g_1'-g_2'-Pe_1Pe_2)(Pe_1+Pe_2)^2/16-3(Pe_1+Pe_2)^4/256.$$

Likewise, Eqs. (26) and (27) admit the following steady-state analytical expressions for the dimensionless concentration distributions in the aquitard and lower aquifer, respectively, as

$$C_{aD}=\frac{(\exp(Pe_a z_D)-\exp(-Pe_a))C_{1D}+(1-\exp(Pe_a z_D))C_{2D}}{1-\exp(-Pe_a)} \quad (30)$$

and

$$C_{2D}=\frac{h_4}{\beta_3(2v_3-Pe_2)}\exp(v_3\cdot x_D)\sin(\beta_3\cdot x_D) \quad (31)$$

When neglecting the advective term in the aquitard and assuming that the aquitard thickness extends to infinity (i.e., $b_a\to\infty$), the upper aquifer can be considered as a single fracture in a rock matrix. As such, the variables h_1, h_2, Λ_1, and Λ_2 are all equal to zero. Eqs. (24) and (26), respectively, can then be reduced to

$$\overline{C}_{1D}(x_D,p)=\frac{1}{p}\exp\left[\left(v_1-\sqrt{v_1^2+\frac{\varepsilon_1}{2}+p}\right)x_D\right] \quad (32)$$

$$\overline{C}_{aD}(z,p)=\overline{C}_{1D}\exp\left(-\frac{z}{b}\sqrt{\frac{R_a D_1}{R_1 D_a}p}\right) \quad (33)$$

Note that Eqs. (32) and (33) are equivalent to the corresponding terms in the solutions of Tang et al. (1981), developed for contaminant transport along a discrete fracture in a porous rock matrix, which is indeed a special case of the present solution.

2.3. Finite difference model

A finite difference model is developed to simulate two-dimensional contaminant transport in an aquifer–aquitard–aquifer system and its simulation result is then used to compare with the present solution. The governing equation for the model can be expressed as

$$\frac{\partial C}{\partial t}=\frac{D_x}{R}\frac{\partial^2 C}{\partial x^2}+\frac{D_z}{R}\frac{\partial^2 C}{\partial z^2}-\frac{v_x}{R}\frac{\partial C}{\partial x}-\frac{v_z}{R}\frac{\partial C}{\partial z} \quad (34)$$

The explicit finite difference approximation for Eq. (34) may be written as

$$\frac{C_{ij}^{n+1}-C_{ij}^n}{\Delta t}=\frac{D_x}{R}\frac{C_{i+1,j}^n-2C_{ij}^n+C_{i-1,j}^n}{(\Delta x)^2}+\frac{D_z}{R}\frac{C_{ij+1}^n-2C_{ij}^n+C_{ij-1}^n}{(\Delta z)^2}-\frac{v_x\Delta z}{R}\times(C_{ij}^n-C_{i-1,j}^n)-\frac{v_z\Delta x}{R}(C_{ij}^n-C_{ij-1}^n)$$

where Δx and Δz are the grid sizes in the x and z directions, respectively, Δt is the time increment, C_{ij}^n is the contaminant concentration at the nodal point (i,j), and time level n. The ordered integer pair (i,j) is a distance $(i-1)\Delta x$ in the positive x direction and $(j-1)\Delta z$ in the negative z direction. In addition, the superscript $n+1$ denotes the time level one step later than the time level n.

3. Results and discussions

Eqs. (24), (26), and (27) comprising hyperbolic functions (e.g., $\sin h(\cdot)$ and $\tan h(\cdot)$) are rather complicated; thus their solutions in the time domain may not be tractable. The inversion routine DINLAP of IMSL (2003), developed based on a numerical algorithm originally proposed by Crump (Crump, 1976; Yang and Yeh, 2005) and later modified by de Hoog et al. (1982), is used to determine the time-domain solutions of those equations. This algorithm approximates Laplace inversion of the inverted function in a Fourier series and accelerates the computation using Shanks method (Yeh and Yang, 2006). Semi-analytical expressions for the concentration distributions in the Laplace domain for the lower aquifer, aquitard, and upper aquifer are numerically inverted using this routine to yield concentration distributions in the real-time domain with accuracy to the sixth decimal.

3.1. Concentration distributions in the aquifer–aquitard system

We consider that the contaminants are well mixed with water and enters the upper aquifer from the inlet boundary continuously. The default parameters for the following study are listed in Table 2. The molecular diffusion coefficient chosen for both the aquifers

and the aquitard (D^*) is set to 1.57×10^{-9} m^2/s. The select average pore velocities (v_x) for the upper and lower aquifer are 1.16×10^{-6} m/s and 1.16×10^{-7} m/s, respectively. The values of the effective diffusion coefficient and average pore velocity of the upper aquifer are adopted from Zhan et al. (2009b). The appropriate average pore velocity of the aquitard is 1.16×10^{-9} m/s. Such a value is reasonable if compared with field scale data given by Cherry et al. (2006) in which they compiled hydrogeologic data from field studies in different unlithified aquitards. Data from laboratory and field experiments in unfractured sandy-silty aquitards in Sweden and Norway indicate that the vertical hydraulic conductivity ranges from 5×10^{-9} to 5×10^{-5} m/s and the porosity is from 0.18 to 0.48. The field-scale dispersivity α_L determined from tracer studies and pump tests (Bedient et al., 1994; Chen et al.,1996) is set to 2 m. Therefore, the corresponding dispersion coefficients for the upper and lower aquifer are 2.32×10^{-6} m^2/s and 2.32×10^{-7} m^2/s, respectively, if ignoring the molecular diffusion. Two different leakage velocities in the aquitard are considered: $v_a = 0$ and 1.16×10^{-9} m/s, corresponding to Peclet numbers Pe_a of 0 and 0.5, respectively. In addition, a default porosity value is set to 0.36 for all units.

Fig. 2 shows the predicted spatial distributions of the dimensionless concentration in the upper and lower aquifers for the cases $Pe_a = 0$ and 0.5 at $t_D = 1$, 5, 10 and ∞ (a steady state). Fig. 2a shows that the penetration distance of contaminant mass in the upper aquifer increases reasonably with elapsed time in the case of $Pe_a = 0$. This figure indicates that the difference in dimensionless concentration obtained from those two cases becomes large when the elapsed time is large due to ignoring the leakage velocity of the aquitard. Fig. 2b demonstrates that the advective transport process in the aquitard drives the contaminant mass through the aquitard. The dimensionless concentration in the lower aquifer increases with the elapsed time. The dimensionless concentration for the case of $Pe_a = 0.5$ is about 17% higher than that of $Pe_a = 0$ at $t_D = 10$, indicating moderate errors in the prediction of contaminant concentration are produced by neglecting the advective transport in the aquitard at large time.

The dimensionless concentrations of contaminant as the function of distance in the aquitard are plotted at various elapsed times shown in Fig. 3. Apparently, the dimensionless concentration at location $x_D = 5$ reaches its steady-state condition approximately at $t_D = 5$ regardless of the presence of aquitard advection or not. It also shows that the dimensionless concentration is lower in the case of $Pe_a = 0$. These results reveal that the leakage velocity of the aquitard has some impact on the dimensionless concentration distribution for contaminant transport in an aquifer–aquitard–aquifer system.

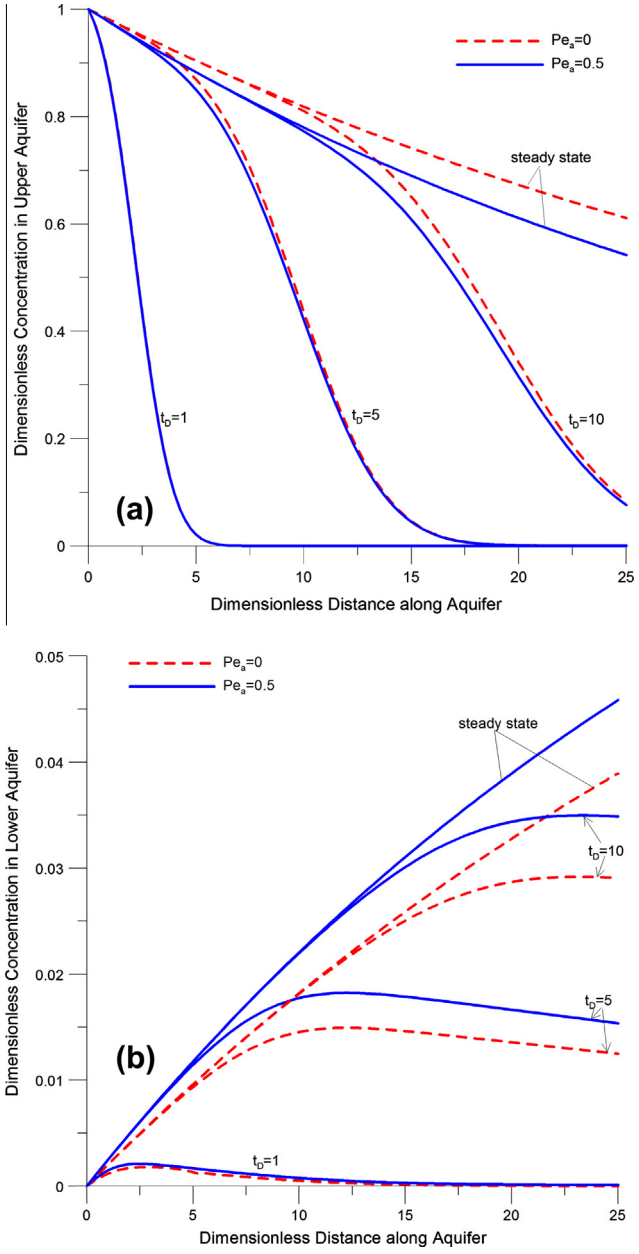

Fig. 2. Spatial distributions of dimensionless concentration in the (a) upper aquifer and (b) lower aquifer at various elapsed times for the cases with different aquitard Peclet numbers.

Table 2
The parameter values for the aquifers and aquitard.

Parameter	Symbol	Default value
Lower and upper aquifer thickness	b_1=b_2=$2b$	4.0 m
Aquitard thickness	b_a	0.5 m
Longitudinal dispersivity of the aquifer	α_L	2 m
Average pore velocity in the aquifer	v_1,v_2	1.16E−6, 1.16E−7 m/s
Average pore velocity in the aquitard	v_a	1.16E−9 m/s
Longitudinal dispersivity of the aquifer	α_L	2.0 m
Longitudinal dispersion coefficient of the aquifer	D_1,D_2	2.32E−6, 2.32E−7 m^2/s
Longitudinal dispersion coefficient of the aquitard	D_a	1.16E−9 m^2/sec
Effective diffusion coefficient	D^*	1.57E−9 m^2/s
Tortuosity of the aquitard	τ	0.74
Porosity	$\theta_1 = \theta_2 = \theta_a$	0.36
Retardation factor	R_1, R_2	1.0
	R_a	1.0, 2.0

Here we examine the contaminant concentration level in the lower aquifer for various aquitard Peclet numbers and elapsed times as shown in Fig. 4. The dimensionless contaminant concentration in the lower aquifer apparently increases with the Peclet number; however, the differences in concentrations for different Peclet numbers are insignificant at early time. Moreover, the contaminant concentration in the lower aquifer will be largely underestimated if neglecting the presence of leakage velocity in the aquitard, i.e., assuming a zero Peclet number.

3.2. Comparisons with finite difference simulation result

Consider a two-dimensional aquifer–aquitard–aquifer system with a thickness of 4 m for the upper and lower aquifers and 0.5 m for the aquitard. The horizontal length of the aquifer system

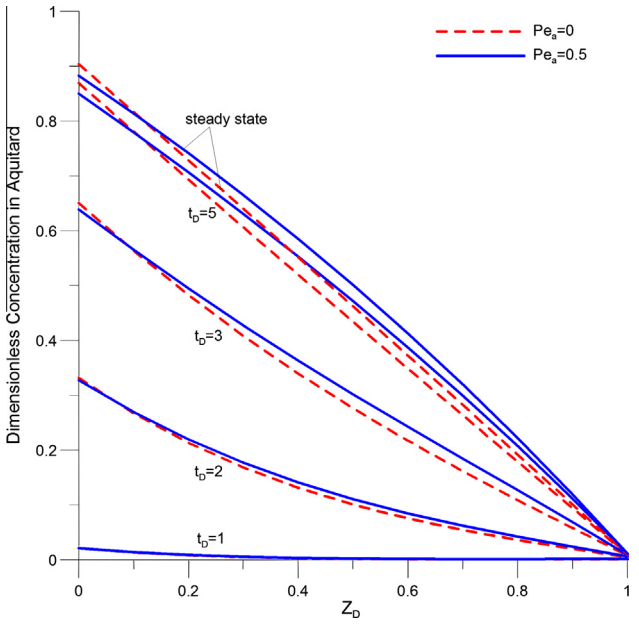

Fig. 3. Dimensionless concentration distributions in the aquitard along the vertical axis at various elapsed times and $x_D = 5$ for the cases with different aquitard Peclet numbers.

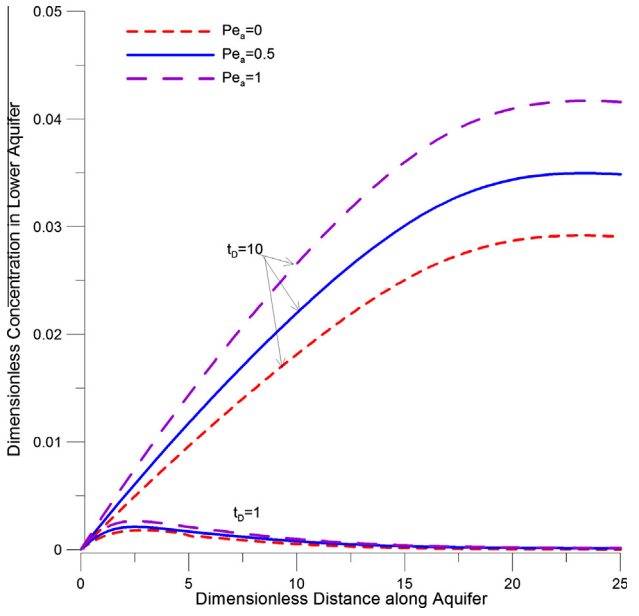

Fig. 4. Comparisons of dimensionless concentration distributions in the lower aquifer with different aquitard Peclet numbers at various elapsed times.

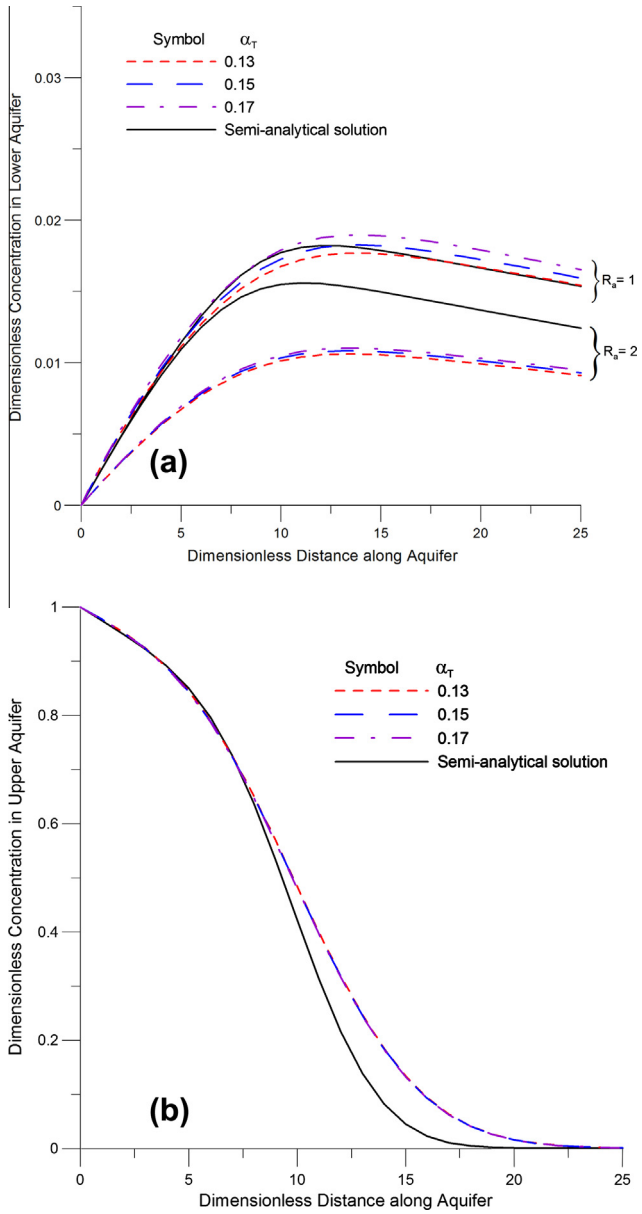

Fig. 5. Spatial distributions of dimensionless concentration predicted by the present solution and depth-averaged finite difference solution in the (a) lower aquifer and (b) upper aquifer at dimensionless elapsed time of $t_D = 5$.

is 120 m. The grid size for Δx and Δz are chosen as 1 m and 0.1 m, respectively, and Δt is set as 0.05 day in the finite difference simulations. In other words, this aquifer–aquitard–aquifer system with a domain of 120 m by 8.5 m is discretized into a 120 by 85 finite difference grids. The values of the model parameters assigned to the block-centered nodes given in Table 2 are identical to those used in the present solution. Additionally, various values of the transverse dispersivity α_T (m) with the aquitard retardation factor R_a of 1 and 2 are used in the numerical simulations and compared with the concentration distributions predicted from the present solution.

In order to compare the spatial concentration distributions predicted by the present solution with finite difference solution, the depth-averaged concentrations are taken over the entire vertical direction for both upper and lower aquifers. Fig. 5a and b show the spatial concentration distributions as the function of distance in the lower and upper aquifers, respectively, along the x-direction at elapsed time $t_D = 5$ (i.e., $t = 4000$ days). Fig. 5a reveals that the present solution is slightly different from the finite difference solution when considering the transverse dispersivity of 0.15 m in the upper aquifer with the aquitard retardation factor of unity. Obviously, a larger retardation factor provides better protection to its adjacent aquifer from contamination than a smaller one. The results also indicate that the contaminant concentration in the aquitard is largely retarded by sorption. The depth-averaged concentrations in the upper aquifer, as shown in Fig. 5b, are however all very close and slightly differ from the present solution in the cases of the transverse dispersivity varying from 0.13 m to

0.17 m. To verify the accuracy, relative differences of the present solution with the simulated and depth- averaged results from the two-dimensional finite difference solution are subsequently calculated. The largest relative difference between the present solution and finite difference model for the lower aquifer are 4% at $x_D = 20$ in the case of $\alpha_T = 0.15$ m and $R_a = 1$. For the case of $R_a = 2$, however, the relative difference increases to 26%, which shows the estimated concentration by numerical simulation is lower than that by the semi-analytical solution. This discrepancy may come from two facts. One is that both the vertical advective and dispersive fluxes in the lower and upper aquifers are not considered in the present solution. The other may be caused by the numerical errors introduced at the aquifer–aquitard interfaces due to the drastic change of aquifer parameters and concentration gradients near the aquifer–aquitard interfaces (Zhan et al., 2009a).

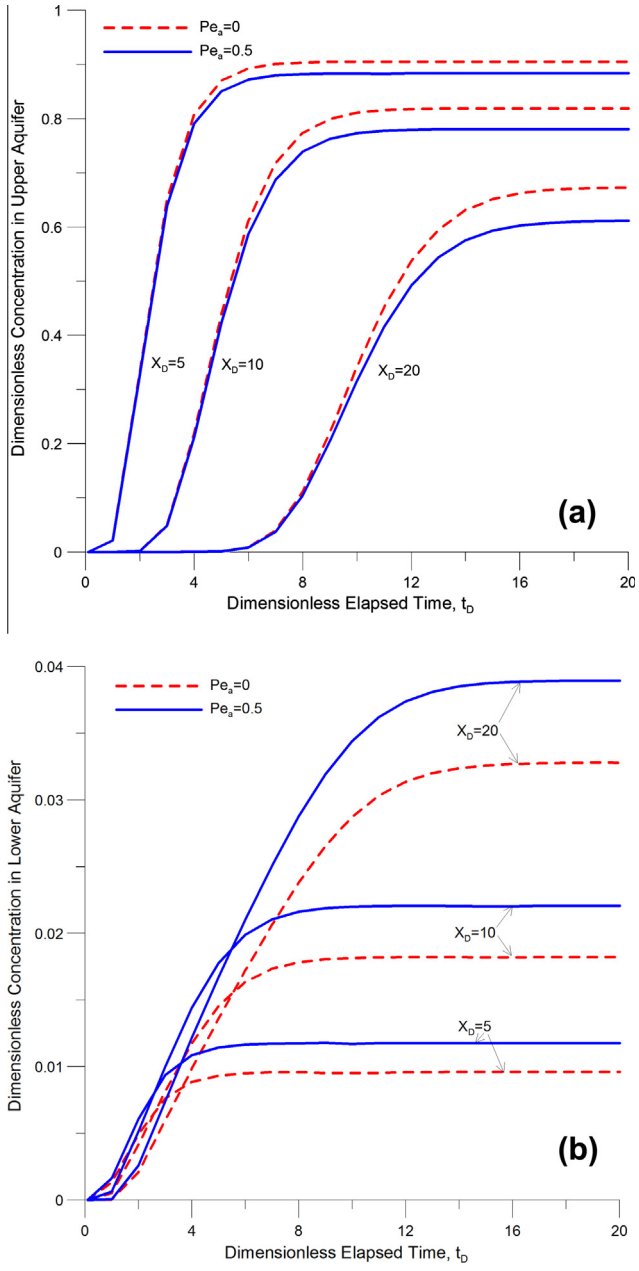

Fig. 6. Temporal distributions of dimensionless concentration in the (a) upper aquifer and (b) lower aquifer at different locations for the cases with different aquitard Peclet numbers.

3.3. Breakthrough curves in the aquifer

Fig. 6 provides further analysis of the effect of the aquitard's Peclet number on the contaminant migration in the two-aquifer system. Fig. 6a presents the variation in the temporal distribution curves of dimensionless concentration in the upper aquifer at different observation locations (i.e., $x_D = 5$, 10, and 20). It is seen that the dimensionless concentration in the upper aquifer increases with elapsed time and the contaminant concentration leaked from the aquitard is deeply affected by the leakage velocity. Fig. 6b shows the temporal distributions of dimensionless concentration in the lower aquifer observed at different locations. When the flow system reaches its steady-state condition, the dimensionless concentration of contaminant in the lower aquifer is 0.022 while that in the upper one is about 0.781 at $x_D = 10$ when $Pe_a = 0.5$. In comparison, the dimensionless concentration is 0.018 in the lower aquifer and 0.819 in the upper aquifer when ignoring the presence of leakage velocity at the aquitard ($Pe_a = 0$). Those results indicate that the aquitard advection has some influence on the advance of the contaminant front to the lower aquifer.

4. Conclusions

This study deals with the issue of one-dimensional contaminant transport in an aquifer–aquitard–aquifer system. A mathematical model has been developed under the consideration of leakage velocity in the aquitard. The Laplace-domain solution of the model is derived by the technique of Laplace transforms and its time-domain solution is obtained from de Hoog et al.'s method. This solution is used to analyze the effects of leakage velocity in the aquitard as well as advective–dispersive transport in the aquifers on the contaminant concentration distributions in aquifer–aquitard–aquifer systems. In addition, an explicit finite difference model is also developed to simulate two-dimensional contaminant transport in the two-aquifer system. The relative differences in concentration distributions predicted by the present solution and the depth-averaged concentrations of the finite difference solutions are small. The deviations between those two solutions are mainly due to the neglect of the vertical advective and dispersive fluxes in the lower and upper aquifers in the present solution.

The influence of diffusion and advection on the migration of contaminant in the aquitard and adjacent aquifers is also investigated. When the diffusion process in the aquitard is significant, the penetration distance of the contaminant in the upper aquifer is considerably increased with elapsed time. Meanwhile, the contamination through the lower aquifer from the aquitard is moderately reduced compared with that when the contaminant transport in the aquitard takes place by both diffusion and advection.

Advection in the aquitard is very likely to occur in most stratified porous media once there is a head gradient existed between the aquifers. It is found that some prediction errors may be introduced in such a two-aquifer system if ignoring the advective flux in the aquitard.

Acknowledgements

This study was partially supported by the Taiwan National Science Council under Grant numbers NSC 99-2221-E-009-062-MY3 and NSC 101-2221-E-009-105-MY2. The authors would like to thank three anonymous reviewers for their valuable and constructive comments.

Appendix A. Development of Laplace-domain solution of the present model

The solution of the contaminant transport equation is often obtained by the techniques of Laplace transform. Taking the Laplace transform of the concentration $C_i(x,t)$ leads to

$$L[C_i(x,t)] = \int_0^\infty C_i(x,t)e^{-st}dt = \overline{C}_i(x,p) \tag{A1}$$

Eqs. (1)–(14) can be expressed in dimensionless forms using dimensionless parameters given in Table 1. After taking the Laplace transform, the dimensionless transport Eq. (6) becomes

$$\frac{d^2\overline{C}_{aD}}{dz_D^2} - Pe_a\frac{d\overline{C}_{aD}}{dz_D} = \delta_1 p\overline{C}_{aD} \tag{A2}$$

The general solution of Eq. (A2) can be written as

$$\overline{C}_{aD}(x_D,z_D,p) = \exp(v_0 z_D)\cdot[A_1(x_D,p)\exp(\beta_0 z_D) + A_2(x_D,p) \times \exp(-\beta_0 z_D)] \tag{A3}$$

where $v_0 = Pe_a/2$; $\beta_0 = \sqrt{v_0^2+\delta_1 p}$; and coefficients A_1 and A_2 which are independent of z_D should be determined by the boundary conditions.

The Laplace transform of Eqs. (8) and (9) in dimensionless forms are, respectively, given by

$$\overline{C}_{aD}(x_D,0,p) = \overline{C}_{1D}(x_D,p) \tag{A4}$$

and

$$\overline{C}_{aD}(x_D,-1,p) = \overline{C}_{2D}(x_D,p) \tag{A5}$$

The coefficients A_1 and A_2 are determined from substituting Eqs. (A4) and (A5) into Eq. (A3), respectively, as

$$A_1(x_D,p) = \frac{\overline{C}_{2D} - \overline{C}_{1D}\exp(-v_0)\exp(\beta_0)}{\exp(-v_0)(\exp(-\beta_0)-\exp(\beta_0))} \tag{A6}$$

and

$$A_2(x_D,p) = \frac{\overline{C}_{1D}\exp(-v_0)\exp(-\beta_0) - \overline{C}_{2D}}{\exp(-v_0)(\exp(-\beta_0)-\exp(\beta_0))} \tag{A7}$$

The substitution of Eqs. (A6) and (A7) into Eq. (A3) admits the dimensionless result for concentration distribution in the aquitard as

$$\overline{C}_{aD}(x_D,z_D,p) = \frac{\exp(v_0 z_D)}{\sin h(\beta_0)}\{\sin h(\beta_0(1+z_D))\overline{C}_{1D} - \exp(v_0) \times \sin h(\beta_0 z_D)\overline{C}_{2D}\} \tag{A8}$$

In addition, it follows from taking Laplace transform of Eq. (1) with the flux term defined by Eq. (2) in dimensionless form that

$$\frac{d^2\overline{C}_{1D}}{dx_D^2} - Pe_1\frac{d\overline{C}_{1D}}{dx_D} - \varepsilon_1\overline{C}_{1D} + \kappa_1\left.\frac{d\overline{C}_{aD}}{dz_D}\right|_{z_D=0} - p\overline{C}_{1D} = 0 \tag{A9}$$

subject to the boundary conditions

$$\overline{C}_{1D}(0,p) = \frac{1}{p} \tag{A10}$$

$$\overline{C}_{1D}(\infty,p) = 0 \tag{A11}$$

The concentration gradient at the interface between the upper aquifer and aquitard, i.e., at $z_D = 0$, can be obtained as

$$\left.\frac{d\overline{C}_{aD}}{dz_D}\right|_{z_D=0} = \left(v_0 + \frac{\beta_0}{\tan h(\beta_0)}\right)\overline{C}_{1D} - \left(\frac{\beta_0\exp(v_0)}{\sin h(\beta_0)}\right)\overline{C}_{2D} \tag{A12}$$

Substituting Eq. (A12) into Eq. (A9) results in the following equation for $\overline{C}_{1D}(x_D,p)$:

$$\frac{d^2\overline{C}_{1D}}{dx_D^2} - Pe_1\frac{d\overline{C}_{1D}}{dx_D} - g_1\overline{C}_{1D} = h_1\overline{C}_{2D} \tag{A13}$$

where $g_1 = \varepsilon_1/2 - \kappa_1\beta_0/\tan h(\beta_0) + p$ and $h_1 = \kappa_1\beta_0\exp(v_0)/\sin h(\beta_0)$. Since Eq. (A13) is a linear second-order ordinary differential equation (ODE), it can be solved by applying the superposition principle. The Laplace-domain solution of Eq. (A13) can therefore be expressed as the sum of a homogeneous solution $\overline{C}_{1D}^h$ and a non-homogeneous solution $\overline{C}_{1D}^p$:

$$\overline{C}_{1D}(x_{1D},p) = \overline{C}_{1D}^h(x_D,p) + \overline{C}_{1D}^p(x_D,p) \tag{A14}$$

The general solution of homogeneous equation Eq. (A13) can be found as

$$\overline{C}_{1D}^h(x_D,p) = \exp(v_1 x_D)\{B_1\exp(\beta_1 x_D) + B_2\exp(-\beta_1 x_D)\} \tag{A15}$$

where $v_1 = Pe_1/2$; $\beta_1 = \sqrt{v_1^2+g_1}$; B_1 and B_2 are undetermined constants.

The non-homogeneous solution of Eq. (A13) can be obtained as

$$\overline{C}_{1D}^p(x_D,p) = \frac{h_1}{2\beta_1}\int_0^{x_D}\overline{C}_{2D}(\xi,p)\{\exp((x_D-\xi)(v_1-\beta_1)) - \exp((x_D-\xi)(v_1+\beta_1))\}d\xi \tag{A16}$$

Substituting Eqs. (A15) and (A16) into Eq. (A14), the general solution for the upper aquifer in the Laplace-domain has the form

$$\overline{C}_{1D}(x_D,p) = B_1\exp(s_1x_D) + B_2\exp(s_2x_D) + \frac{h_1}{s_2-s_1} \times \int_0^{x_D}\overline{C}_{2D}(\xi,p)\{\exp((x_D-\xi)s_2) - \exp((x_D-\xi)s_1)\}d\xi \tag{A17}$$

where $s_1 = v_1+\beta_1$ and $s_2 = v_1-\beta_1$.

Furthermore, for the concentration distribution in the lower aquifer, after taking the Laplace transform to Eq. (10) with the flux term defined by Eq. (11) in dimensionless form it follows that

$$\frac{d^2\overline{C}_{2D}}{dx_D^2} - Pe_2\frac{d\overline{C}_{2D}}{dx_D} + \varepsilon_2\overline{C}_{2D} - \kappa_2\left.\frac{d\overline{C}_{aD}}{dz_D}\right|_{z_D=-1} - \delta_2 p\overline{C}_{2D} = 0 \tag{A18}$$

subject to the boundary conditions

$$\overline{C}_{2D}(0,p) = 0 \tag{A19}$$

$$\overline{C}_{2D}(\infty,p) = 0 \tag{A20}$$

The concentration gradient at the interface between lower aquifer and aquitard, i.e., at $z_D = -1$, can be expressed as

$$\left.\frac{d\overline{C}_{aD}}{dz_D}\right|_{z_D=-1} = \frac{\beta_0\exp(-v_0)}{\sin h(\beta_0)}\overline{C}_{1D} + \left(v_0 - \frac{\beta_0}{\tan h(\beta_0)}\right)\overline{C}_{2D} \tag{A21}$$

Substituting Eq. (A21) into Eq. (A18) results in the following equation for $\overline{C}_{2D}(x_D,p)$:

$$\frac{d^2\overline{C}_{2D}}{dx_D^2} - Pe_2\frac{d\overline{C}_{2D}}{dx_D} + g_2\overline{C}_{2D} = h_2\overline{C}_{1D} \tag{A22}$$

where $g_2 = \varepsilon_2/2 + \kappa_2\beta_0/\tan h(\beta_0) - \delta_2 p$ and $h_2 = \kappa_2\beta_0\exp(-v_0)/\sin h(\beta_0)$.

Substituting Eq. (A17) into Eq. (A22), the governing equation for the lower aquifer can be rearranged as

$$\frac{d^2\overline{C}_{2D}}{dx_D^2} - Pe_2\frac{d\overline{C}_{2D}}{dx_D} + g_2\overline{C}_{2D} - \frac{h_1h_2}{s_2-s_1}\int_0^{x_D}\overline{C}_{2D}(\xi,p)\{\exp((x_D-\xi)s_2) - \exp((x_D-\xi)s_1)\}d\xi = h_2\{B_1\exp(s_1x_D) + B_2\exp(s_2x_D)\} \tag{A23}$$

Taking the derivative of Eq. (A23) with respect to x_D leads to

$$\frac{d^3\overline{C}_{2D}}{dx_D^3} - Pe_2\frac{d^2\overline{C}_{2D}}{dx_D^2} + g_2\frac{d\overline{C}_{2D}}{dx_D} - \frac{h_1h_2}{s_2-s_1}\begin{pmatrix} s_2\exp(s_2x_D)\int_0^{x_D}\overline{C}_2(\xi,p)\exp(-s_2\xi)d\xi \\ -s_1\exp(s_1x_D)\int_0^{x_D}\overline{C}_2(\xi,p)\exp(-s_1\xi)d\xi \end{pmatrix} = h_2\{B_1s_1\exp(s_1x_D) + B_2s_2\exp(s_2x_D)\}$$

A third-order ODE for the upper aquifer is obtained by subtracting Eq. (A24) from Eq. (A23) and multiplying it by s_1 as

$$\frac{d^3\overline{C}_{2D}}{dx_D^3} - (Pe_2+s_1)\frac{d^2\overline{C}_{2D}}{dx_D^2} + (g_2+Pe_2s_1)\frac{d\overline{C}_{2D}}{dx_D} - s_1g_2\overline{C}_{2D} - h_1h_2\exp(s_2x_D)\int_0^{x_D}\overline{C}_2(\xi,p)\exp(-s_2\xi)d\xi = h_2B_2(s_2-s_1)\exp(s_2x_D) \quad (A25)$$

Taking the derivative of Eq. (A25) with respect to x_D results in

$$\frac{d^4\overline{C}_{2D}}{dx_D^4} - (Pe_2+s_1)\frac{d^3\overline{C}_{2D}}{dx_D^3} + (g_2+Pe_2s_1)\frac{d^2\overline{C}_{2D}}{dx_D^2} - s_1g_2\frac{d\overline{C}_{2D}}{dx_D} - h_1h_2\begin{pmatrix} s_2\exp(s_2x_D)\int_0^{x_D}\overline{C}_2(\xi,p)\exp(-s_2\xi)d\xi \\ +\exp(s_2x_D)\overline{C}_2(x_D,p)\exp(-s_2x_D) \end{pmatrix} = h_2B_2(s_2-s_1)s_2\exp(s_2x_D) \quad (A26)$$

Similarly, subtracting Eq. (A26) from Eq. (A25) and multiplying it by s_2 yields a fourth-order ODE for the upper aquifer expressed as

$$\frac{d^4\overline{C}_{2D}}{dx_D^4} - (Pe_1+Pe_2)\frac{d^3\overline{C}_{2D}}{dx_D^3} - (g_1-g_2-Pe_1Pe_2)\frac{d^2\overline{C}_{2D}}{dx_D^2} - (Pe_1g_2-Pe_2g_1)\frac{d\overline{C}_{2D}}{dx_D} - (g_1g_2+h_1h_2)\overline{C}_{2D} = 0 \quad (A27)$$

The characteristic equation of Eq. (A27) can then be expressed as (Kreyszig, 1979, p. 104)

$$\lambda^4 + d\lambda^3 + e\lambda^2 + f\lambda + l = 0 \quad (A28)$$

where λ is an undetermined constant; $d = -(Pe_1 + Pe_2)$; $e = g_2 - g_1 + Pe_1Pe_2$; $f = Pe_2g_1 - Pe_1g_2$; $l = -g_1g_2 - h_1h_2$. Assuming $y = \lambda + d/4$ and substituting it into Eq. (A28) results in

$$y^4 + o_1y^2 = -q_1y - r_1 \quad (A29)$$

where $o_1 = e - 3d^2/8$; $q_1 = f - ed/2 + (d/2)^3$; $r_1 = l - fd/4 + e(d/4)^2 - 3(d/4)^4$.

Eq. (A29) can be reduced to a cubic equation by applying Ferrari's solution (Korn and Korn, 2000, p. 24). Adding $(\delta/2)^2$ to Eq. (A29) in both sides yields

$$\left(y^2+\frac{\delta}{2}\right)^2 = (\delta-o_1)y^2 - q_1y + \left(\frac{\delta}{2}\right)^2 - r_1 \quad (A30)$$

Note that the left-hand side of Eq. (A30) is a perfect square. If the right-hand side of Eq. (A30) is also a perfect square, then its discriminant will be zero. That is $q_1^2 - (\delta - o_1)(\delta^2 - 4r_1) = 0$ or

$$\delta^3 - o_1\delta^2 - 4r_1\delta + (4o_1r_1 - q_1^2) = 0 \quad (A31)$$

Then setting $U = \delta - o_1/3$ and substituting it into Eq. (A31) leads to

$$U^3 + o_2U + q_2 = 0 \quad (A32)$$

where $o_2 = -(4r_1 + o_1^2/3)$ and $q_2 = 8r_1o_1/3 - 2(o_1/3)^3 - q_1^2$.

Eq. (A32) can further be reduced to two quardratic equations by Cardan's solution (Korn and Korn, 2000, p. 23) as

$$U = \left(-\frac{q_2}{2} + \sqrt{\left(\frac{q_2}{2}\right)^2 + \left(\frac{o_2}{3}\right)^3}\right)^{1/3} + \left(-\frac{q_2}{2} - \sqrt{\left(\frac{q_2}{2}\right)^2 + \left(\frac{o_2}{3}\right)^3}\right)^{1/3}$$

or

$$\delta = \left(-\frac{q_2}{2} + \sqrt{\left(\frac{q_2}{2}\right)^2 + \left(\frac{o_2}{3}\right)^3}\right)^{1/3} + \left(-\frac{q_2}{2} - \sqrt{\left(\frac{q_2}{2}\right)^2 + \left(\frac{o_2}{3}\right)^3}\right)^{1/3} + \frac{o_1}{3} \quad (A33)$$

Accordingly, Eq. (A30) can be rewritten as.

$$\left(y^2+\frac{\delta}{2}\right)^2 = (\delta-o_1)\left(y - \frac{q_1}{2(\delta-o_1)}\right)^2 \quad (A34)$$

which is indeed a quadratic equation and implies that it can be solved by the method of Completing the Square. This transforms the problem of finding the four roots of the quartic equation to that of determining the roots of following two quadratic equations.

$$y^2 + \frac{\delta}{2} = \pm\sqrt{\delta-o_1}\left(y - \frac{q_1}{2(\delta-o_1)}\right) \quad (A35)$$

The general solution of the lower aquifer with four undetermined coefficients can then be obtained as

$$\overline{C}_{2D}(x_D,p) = \exp\left(\left(\frac{\sqrt{\mu}}{2} - \frac{d}{4}\right)x_D\right)\left(E_1\cos\frac{\sqrt{\mu+2o_1+2q_1\mu^{-1/2}}}{2}x_D + E_2\sin\frac{\sqrt{\mu+2o_1+2q_1\mu^{-1/2}}}{2}x_D\right) + \exp\left(-\left(\frac{\sqrt{\mu}}{2} + \frac{d}{4}\right)x_D\right)\left(E_3\cos\frac{\sqrt{\mu+2o_1-2q_1\mu^{-1/2}}}{2}x_D + E_4\sin\frac{\sqrt{\mu+2o_1-2q_1\mu^{-1/2}}}{2}x_D\right) \quad (A36)$$

where

$$\mu = \left(-\frac{q_2}{2} + \sqrt{\left(\frac{q_2}{2}\right)^2 + \left(\frac{o_2}{3}\right)^3}\right)^{1/3} + \left(-\frac{q_2}{2} - \sqrt{\left(\frac{q_2}{2}\right)^2 + \left(\frac{o_2}{3}\right)^3}\right)^{1/3} - \frac{2o_1}{3} \quad (A37)$$

and E_1, E_2, E_4, and E_4 are undetermined coefficients.

From the boundary conditions of Eqs. (A19) and (A20), E_1, E_2, and E_3 are then zero. The general solution for the lower aquifer can thus be reduced to

$$\overline{C}_{2D}(x_D,p) = E_4\exp(v_2x_D)\sin(\beta_2x_D) \quad (A38)$$

where $v_2 = (Pe_1 + Pe_2 - 2\sqrt{\mu})/4$ and $\beta_2 = \sqrt{\mu + 2o_1 - 2q_1\mu^{-1/2}}$.

Substituting Eq. (A38) into Eq. (A22) and incorporated with the boundary conditions of Eqs. (A10) and (A19), E_4 can be determined as

$$E_4 = \frac{h_2}{\beta_2(2v_2 - Pe_2)p} \quad (A39)$$

Finally, the solution for the lower aquifer in the Laplace domain can be found as

$$\overline{C}_{2D}(x_D,p) = \frac{h_2}{\beta_2(2v_2 - Pe_2)p}\exp(v_2x_D)\sin(\beta_2x_D) \quad (A40)$$

Similarly, substituting Eq. (A40) into Eq. (A17) subject to the boundary conditions, Eqs. (A10) and (A11), the general solution for the upper aquifer in the Laplace-domain can be obtained as

$$\overline{C}_{1D}(x_D,p) = \frac{(1+\Lambda_1)}{p}\exp(s_2x_D) - \frac{\Lambda_1\cos(\beta_2x_D) - \Lambda_2\sin(\beta_2x_D)}{p}\exp(v_2x_D) \quad (A41)$$

with

$$\Lambda_1 = \frac{h_1 h_2}{(\beta_2^2+(\nu_2-s_1)^2)(\beta_2^2+(\nu_2-s_2)^2)} \cdot \frac{2\nu_2 - Pe_1}{2\nu_2 - Pe_2}$$

$$\Lambda_2 = \frac{h_1 h_2}{(\beta_2^2+(\nu_2-s_1)^2)(\beta_2^2+(\nu_2-s_2)^2)} \frac{\nu_2(\nu_2 - Pe_1) - \beta_2^2 - g_1}{\beta_2(2\nu_2 - Pe_2)}$$

Appendix B. Development of steady-state solution

The steady-state solution can be obtained from the Laplace-domain solution by applying the Tauberian theorem as

$$C_i(x,\infty) = \lim_{p\to 0} p\overline{C}_i(x,p) \tag{B1}$$

Accordingly, substituting Eq. (24) into Eq. (B1) results in

$$C_{1D}(x,\infty) = \lim_{p\to 0}((1+\Lambda_1(p))\exp(s_2 x_D) - (\Lambda_1(p)\cos(\beta_2 x_D) - \Lambda_2(p)\sin(\beta_2 x_D))\exp(\nu_2 x_D)) \tag{B2}$$

In the limit of Eq. (25) as $p \to 0$, one has

$$\Omega_1 = \frac{h_3 h_4}{(\beta_3^2+(\nu_3-s_3)^2)(\beta_3^2+(\nu_3-s_4)^2)} \cdot \frac{2\nu_3 - Pe_1}{2\nu_3 - Pe_2}$$

$$\Omega_2 = \frac{h_3 h_4}{(\beta_3^2+(\nu_3-s_3)^2)(\beta_3^2+(\nu_3-s_4)^2)} \cdot \frac{\nu_3(\nu_3 - Pe_1) - \beta_3^2 - g_3}{\beta_3(2\nu_3 - Pe_2)}$$

The steady-state solution for the upper aquifer can be determined by substituting Eq. (B3) into Eq. (B2) as

$$C_{1D} = (1+\Omega_1)\exp(s_4 x_D) - [\Omega_1\cos(\beta_3 x_D) - \Omega_2\sin(\beta_3 x_D)] \times \exp(\nu_3 x_D) \tag{B4}$$

Similarly, substituting Eqs. (26) and (27) into Eq. (B1) leads the steady-state solutions for the aquitard and lower aquifer to the forms of Eqs. (30) and (31), respectively.

References

Bedient, P.B., Rifai, H.S., Newell, C.J., 1994. Ground Water Contamination: Transport and Remediation. PTR Prentice Hall, Englewood Cliffs, New Jersey.

Chapman, S.W., Parker, B.L., 2005. Plume persistence due to aquitard back diffusion following dense nonaqueous phase liquid removal or isolation. Water Resour. Res. 41, W12411. http://dx.doi.org/10.1029/2005WR004224.

Chen, J.S., Liu, C.W., Chen, C.S., Yeh, H.D., 1996. A Laplace transform solution for tracer tests in a radially convergent flow field with upstream dispersion. J. Hydrol. 183, 263–275.

Cherry, J.A., Parker, B.L., Bradbury, K.R., Eaton, T.T., Gotkowitz, M.B., Hart, D.J., Borchardt, M.A., 2006. Contaminant Transport Through Aquitards: A State of Science Review. Awwa Research Foundation, Denver, CO 80235-3098.

Crump, K.S., 1976. Numerical inversion of Laplace transforms using a Fourier series approximation. J. Assoc. Comput. Mach. 23 (1), 89–96.

de Hoog, F.R., Knight, J.H., Stokes, A.N., 1982. An improved method for numerical inversion of Laplace transforms, Society for Industrial and Applied Mathematics. J. Sci. Stat. Comput. 3 (3), 357–366.

Freeze, R.A., Cherry, J.A., 1979. Groundwater. Prentice-Hall, Inc., Englewood Cliffs, NJ 07632.

Hantush, M.S., Jacob, C.E., 1955. Non-steady radial flow in an infinite leaky aquifer. Trans. AGU 36, 95–100.

Hunt, B., Scott, D., 2007. Flow to a well in a two-aquifer system. J. Hydrol. Eng. 12 (2), 146–155.

IMSL Fortran Library User's Guide Math/Library, 2003. Visual Numerics, vol. 2 of 2. Version 5.0, Houston, Texas.

Johns, R.A., Roberts, P.V., 1991. A solute transport model for channelized flow in a fracture. Water Resour. Res. 27 (8), 1797–1808.

Johnson, R.L., Cherry, J.A., Pankow, J.F., 1989. Diffusive contaminant transport in natural clay: a field example and implications for clay-lined waste disposal sites. Environ. Sci. Technol. 23, 340–349.

Korn, G.A., Korn, T.M., 2000. Mathematical Handbook for Scientists and Engineers: Definitions, Theorems, and Formulas for Reference and Review. Dover Publications.

Kreyszig, E., 1979. Advanced Engineering Mathematics, forth ed. John Wiley & Sons, New York.

Liu, C.X., Ball, W.P., 2002. Back diffusion of chlorinated solvent contaminants from a natural aquitard to a remediated aquifer under well-controlled field conditions: predictions and measurements. Ground Water 40, 175–184.

Liu, C.T., Yeh, H.D., 2003. Radionuclide transport in multiple and parallel fractured system. Nucl. Technol. Am. Nucl. Soc. 143 (3), 322–334.

Liu, H.H., Bodvarsson, G.S., Zhang, G., 2004. The scale-dependency of the effective matrix diffusion coefficient. Vadose Zone J. 3 (1), 312–315.

Neuman, S.P., Witherspoon, P.A., 1969. Application of current theories of flow in leaky aquifers. Water Resour. Res. 5 (4), 817–829.

Parker, B.L., Cherry, J.A., Chapman, S.W., 2004. Field study of TCE diffusion profiles below DNAPL to access aquitard integrity. J. Contam. Hydrol. 74 (1–4), 197–230.

Tang, D.H., Frind, E.O., Sudicky, E.A., 1981. Contaminant transport in fractured porous media: analytical solution for a single fracture. Water Resour. Res. 17 (3), 555–564.

Yang, S.Y., Yeh, H.D., 2005. Laplace-domain solutions for radial two-zone flow equations under the conditions of constant-head and partially penetrating well. J. Hydraul. Eng., ASCE 131 (3), 209–216. http://dx.doi.org/10.1061/(ASCE)0733-9429(2005) 131:3, 209.

Yeh, H.D., Wang, C.T., 2007. Wang, large-time solutions for groundwater flow problems using the relationship of small p versus large t. Water Resour. Res. 43 (6), W06502. http://dx.doi.org/10.1029/2006WR005472.

Yeh, H.D., Yang, S.Y., 2006. A novel analytical solution for constant-head test in a patchy aquifer. Int. J. Numer. Anal. Met. Geomech. 30 (12), 1213–1230. http://dx.doi.org/10.1002/nag.523.

Zhan, H., Wen, Z., Huang, G., Sun, D., 2009a. Analytical solution of two-dimensional solute transport in an aquifer–aquitard system. J. Contam. Hydrol. 107, 162–174.

Zhan, H., Wen, Z., Gao, G., 2009b. An analytical solution of two-dimensional reactive solute transport in an aquifer–aquitard system. Water Resour. Res. 45, W10501. http://dx.doi.org/10.1029/2008WR007479.

Zlotnik, V.A., Zhan, H., 2005. Aquitard effect on drawdown in water table aquifers. Water Resour. Res. 41, W06022. http://dx.doi.org/10.1029/2004WR003716.